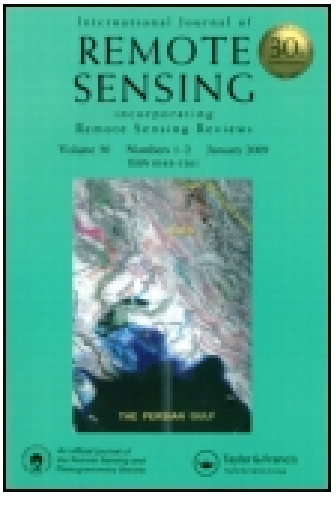

International Journal of Remote Sensing
Publication details, including instructions for authors and subscription information:
http://www.tandfonline.com/loi/tres20

Mapping freshwater marsh species distributions using WorldView-2 high-resolution multispectral satellite imagery

Melissa Vernon Carle[a], Lei Wang[b] & Charles E. Sasser[a]
[a] Department of Oceanography and Coastal Sciences, Louisiana State University, Baton Rouge, LA 70803, USA
[b] Department of Geography and Anthropology, Louisiana State University, Baton Rouge, LA 70803, USA
Published online: 01 Jul 2014.

To cite this article: Melissa Vernon Carle, Lei Wang & Charles E. Sasser (2014) Mapping freshwater marsh species distributions using WorldView-2 high-resolution multispectral satellite imagery, International Journal of Remote Sensing, 35:13, 4698-4716, DOI: 10.1080/01431161.2014.919685

To link to this article: http://dx.doi.org/10.1080/01431161.2014.919685

International Journal of Remote Sensing, 2014
Vol. 35, No. 13, 4698–4716, http://dx.doi.org/10.1080/01431161.2014.919685

Taylor & Francis
Taylor & Francis Group

Mapping freshwater marsh species distributions using WorldView-2 high-resolution multispectral satellite imagery

Melissa Vernon Carle[a]*†, Lei Wang[b], and Charles E. Sasser[a]

[a]*Department of Oceanography and Coastal Sciences, Louisiana State University, Baton Rouge, LA 70803, USA;* [b]*Department of Geography and Anthropology, Louisiana State University, Baton Rouge, LA 70803, USA*

(*Received 24 January 2014; accepted 22 April 2014*)

Freshwater wetlands are highly diverse, spatially heterogeneous, and seasonally dynamic systems that present unique challenges to remote sensing. Maximum likelihood and support vector machine-supervised classification were compared to map wetland plant species distributions in a deltaic environment using high-resolution WorldView-2 satellite imagery. The benefits of the sensor's new coastal blue, yellow, and red-edge bands were tested for mapping coastal vegetation and the eight-band results were compared to classifications performed using band combinations and spatial resolutions characteristic of other available high-resolution satellite sensors. Unlike previous studies, this study found that support vector machine classification did not provide significantly different results from maximum likelihood classification. The maximum likelihood classifier provided the highest overall classification accuracy, at 75%, with user's and producer's accuracies for individual species ranging from 0% to 100%. Overall, maximum likelihood classification of WorldView-2 imagery provided satisfactory results for species distribution mapping within this freshwater delta system and compared favourably to results of previous studies using hyperspectral imagery, but at much lower acquisition cost and greater ease of processing. The red-edge and coastal blue bands appear to contribute the most to improved vegetation mapping capability over high-resolution satellite sensors that employ only four spectral bands.

1. Introduction

Coastal wetlands are valuable resources that provide essential habitat for freshwater, estuarine, and marine species, buffer shorelines, export organic carbon to estuaries, and influence biogeochemical cycles (Nixon 1980; Costanza, Farber, and Maxwell 1989; Hopkinson 1985; Farber 1987; Knutson et al. 1981, 1982). Despite their important ecological role and the value they provide to society, coastal wetlands are threatened by increased populations and development in coastal regions. It has been estimated that worldwide, over one-third of people live within 100 kilometres of the coast (Cohen et al. 1997). In the USA, coastal areas are currently developing more rapidly than any other part of the country (Crossett et al. 2004). Understanding the impact of such development is essential to determine how to best protect existing coastal resources and guide the restoration of degraded ecosystems. Remote sensing provides an opportunity to monitor large-scale patterns and changes to coastal ecological systems that can be difficult

*Corresponding author. Email: mmcarle@hotmail.com
†Present address: National Oceanic and Atmospheric Administration, National Marine Fisheries Service, Office of Habitat Conservation, Restoration Center, 1315 East-West Highway, SSMC3, Silver Spring, MD 20910, USA.

to assess at the field scale, and is thus an extremely valuable tool in guiding the protection and restoration of coastal wetlands.

Coastal wetlands present unique challenges for remote sensing because they are composed of highly diverse mixed vegetation (Adam, Mutanga, and Rugege 2010). This is particularly true of brackish and freshwater marshes, where plant community composition is not as severely limited by salinity stress as in salt marshes (Odum 1988). In addition, annual species are common in tidal freshwater marshes and many of the perennial forbs that inhabit these marshes die back to the sediment each year, creating considerable seasonal and annual variability in the distribution and abundance of individual species (Odum 1988; Pasternack, Hilgartner, and Brush 2000). The phenology of freshwater marsh species commonly results in a seasonal pattern of shifting dominance where perennials are dominant early in the growing season and annuals dominate later in the growing season after the perennials have reached their peak biomass and begun to senesce (Johnson, Sasser, and Gosselink 1985; Odum 1988; Doumlele 1981; Whigham and Simpson 1992; Simpson et al. 1983). In coastal river deltas, this seasonality is further complicated by the spring flood cycle, which controls spring and early summer water levels and thus the timing of species germination and re-sprouting in the early growing season (Johnson, Sasser, and Gosselink 1985).

Many marsh species are spectrally similar to one another, making separation of unique signatures difficult if only a few broad spectral bands are available for classification (Ozesmi and Bauer 2002). The presence of water interspersed with the vegetation dampens the overall reflectance values and further diminishes separability of individual species (Adam, Mutanga, and Rugege 2010; Silva et al. 2008). This factor is further complicated by daily and seasonal changes in water level (Ozesmi and Bauer 2002). Submerged aquatic vegetation, which is common in the understory of emergent wetlands, contributes further spectral confusion.

Most of the earliest attempts to map coastal wetlands involved visual interpretation of colour infrared aerial photography (Ozesmi and Bauer 2002; Adam, Mutanga, and Rugege 2010). Although many of these studies achieved moderate accuracy, particularly with respect to mapping coarse wetland classes, the process is time-intensive and subject to considerable inconsistency related to variability of interpretation and human error (Ozesmi and Bauer 2002). The poor spectral resolution of aerial photography also limits its ability to distinguish the unique spectral responses of individual species (Adam, Mutanga, and Rugege 2010). More recently, remote-sensing researchers have explored automated classification techniques to map wetlands using medium- and high-resolution satellite imagery and satellite and airborne hyperspectral imagery. Although hyperspectral imagery has generally produced the most accurate maps of coastal wetland vegetation, this technology is still relatively expensive and largely inaccessible to coastal wetland managers. High-resolution satellite imagery has been demonstrated to provide classifications that are nearly as accurate at significantly reduced cost.

WorldView-2 (WV-2) is a commercial high spatial resolution satellite that was launched by the company DigitalGlobe in 2009. It provides 2 m imagery in eight spectral bands, including four spectral bands not available in earlier high-resolution multispectral satellite sensors: coastal blue (400–450 nm), yellow (585–625 nm), red-edge (705–745 nm), and a second band in the near-infrared portion of the light spectrum (860–1040 nm). The coastal blue band corresponds to the range of maximum penetration of the water column and is expected to improve bathymetric mapping of shallow coastal environments and submerged vegetation (Marchisio, Pacifici, and Padwick 2010; Collin and Planes 2011; Collin and Hench 2012). The yellow band corresponds to the absorption

range of minor plant pigments that become important in the fall as chlorophyll production drops, and may be valuable for mapping vegetation undergoing stress or senescence (Jensen 2007; Carter 1993; Carter, Cibula, and Miller 1996). The red-edge region of the spectrum represents the transition zone between high absorption by chlorophyll in the red region and high reflection by the spongy mesophyll cells in the near infrared region, and measuring reflectance in this region should improve vegetation classification and estimates of chlorophyll content, biomass, and leaf area index (Jackson 1986; Gates et al. 1965; Gitelson and Merzlyak 1994; Gitelson, Merzlyak, and Lichtenthaler 1996).

In this study, we apply maximum likelihood classification (MLC) and support vector machine (SVM) classification to map freshwater marsh species distributions using WV-2 imagery of a small river delta in coastal Louisiana, USA. The specific objectives of this study are to: (1) evaluate the value of WV-2 high spatial resolution multispectral satellite imagery for monitoring plant community composition in coastal freshwater marshes, (2) compare the use of MLC and SVM classifiers for mapping freshwater marsh vegetation using high-resolution satellite imagery, (3) evaluate the benefit of WV-2's new spectral bands for mapping freshwater marsh vegetation, and (4) compare WV-2 to other available high-resolution satellite sensors for mapping freshwater marsh vegetation.

2. Methods

2.1. Study area

The Wax Lake delta is a naturally evolving young delta of the Atchafalaya River, a major distributary of the Mississippi River in southern Louisiana, USA. It is the product of a diversion of part of the Atchafalaya River through the artificial Wax Lake Outlet and receives approximately one-third of the flow of the Atchafalaya River. The delta emerged from Atchafalaya Bay following record floods in the spring of 1973, and by 1997, the river had built 51.1 km^2 of new land in the Wax Lake delta (Roberts et al. 1997). As new shallow islands emerge, they are colonized by freshwater wetland plants, which trap additional sediments with their roots and increase elevation (Llewellyn and Shaffer 1993; Shaffer et al. 1992). As elevation increases, additional species are able to invade, often displacing the initial colonizing species or limiting them to lower elevations (Johnson, Sasser, and Gosselink 1985; Shaffer et al. 1992). Species richness in the freshwater Wax Lake delta is relatively high compared with other coastal settings, providing a good case study to test the applicability of WV-2 satellite imagery and the use of different classifiers to distinguish between wetland plant species in a spatially heterogeneous landscape.

2.2. Vegetation classes

We used a WV-2 image of the Wax Lake delta taken on 15 October 2011 to map the distribution of freshwater marsh plant species within the delta (Figure 1). The following 17 freshwater marsh species/land-cover classes were included in the classification: trees, *Salix nigra* seedlings, *Colocasia esculenta*, *Polygonum punctatum*, *Bidens laevis*, *Paspalum dissectum*, *Typha* spp., *Phragmites australis*, *Zizaniopsis miliacea*, *Nelumbo lutea*, *Sagittaria* spp., *Potamogeton nodosus*, other submerged aquatic vegetation (SAV), *Eichhornia crassipes*, dead vegetation, water, and bare mudflats. The vegetation classes that were included in the mapping study represent some of the most dominant species in the delta and those that were identified during field reconnaissance.

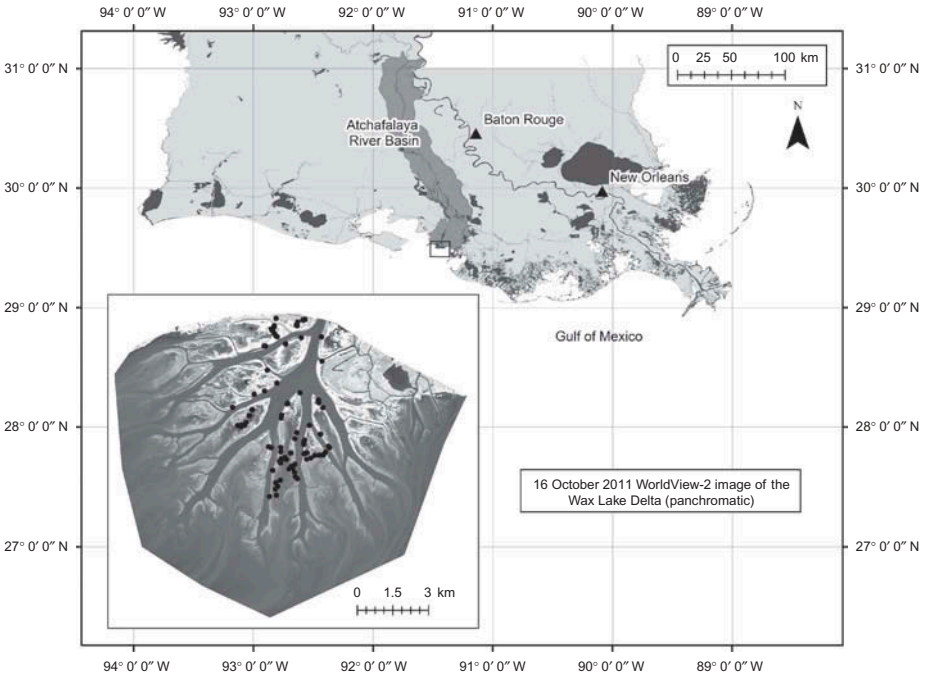

Figure 1. Location of the Wax Lake delta and reference plots used for accuracy assessment.

At the highest elevations, along the natural river levees, the trees class is dominated by *S. nigra* (black willow), a small- to medium-sized tree with multiple trunks and lanceolate leaves (Chabreck and Condrey 1979). Other species of hardwood trees are found growing on dredge spoil disposal levees along the main river channel at the upper end of the delta, but no attempt was made to distinguish between the *S. nigra* and these other tree species for this study. *Colocasia esculenta* (elephant ear or taro) is an invasive perennial forb that grows at slightly lower elevations – along the lower levees on younger islands, down the backside of levees facing the interior of older islands, and in the understory of the willow community. It has large, heart-shaped leaves (up to 0.6 m) with long (1 m) petioles that emanate from a starchy underground corm and can reach a maximum height of 2.5 m with a canopy spread of 2.5 m under ideal growing conditions (Chabreck and Condrey 1979; NRCS 2013). Commonly found interspersed with *C. esculenta* or in mixed communities at high to mid-elevations is *P. punctatum* (dotted smartweed). *Polygonum punctatum* is an annual/perennial herb with branched, trailing stems, linear leaves, and long racemes of scattered white flowers that can grow to a maximum height of about 1 m under ideal growing conditions (NRCS 2013; Chabreck and Condrey 1979).

Intermediate elevations within the delta are dominated by a diverse assemblage of species, many of which are clonal and form large monotypic stands. Included in this group are *B. laevis* (smooth beggartick or bur marigold), *P. dissectum* (mudbank paspalum), *Typha* spp. (cattails), *P. australis* (common reed), and *Z. miliacea* (giant cutgrass). *Bidens laevis* is an annual/perennial herb with an upright, bushy growth form and a maximum height of about 1 m that often forms dense stands in freshwater marshes (Chabreck and Condrey 1979; NRCS 2013). It grows numerous bright yellow flowers in the fall (Chabreck and Condrey 1979). *Paspalum dissectum* is a low-growing perennial

grass that grows to 15–60 cm tall and is locally abundant, forming dense mats in freshwater marshes (Chabreck and Condrey 1979). *Typha* spp. are tall grass-like, perennial herbs that grow from fleshy creeping rhyzomes. The leaves are narrow and erect and grow 1.2–1.8 m tall (Chabreck and Condrey 1979). At least two *Typha* spp. are believed to grow in the Wax Lake delta: *Typha latifolia* (broadleaf cattail) and *Typha angustifolia* (narrowleaf cattail). No attempt was made to distinguish between them for this study. *Phragmites australis* is a tall (2.5–3.4 m), perennial, cane-like grass with stout creeping rhizomes and a plume-like inflorescence that develops in the fall. It typically grows in dense monotypic stands, often expanding outward in a distinct circular pattern (Chabreck and Condrey 1979). *Zizaniopsis miliacea* is a tall, stout perennial grass that grows up to 2.7 m tall under ideal growing conditions and forms dense circular stands in freshwater marshes (Chabreck and Condrey 1979; NRCS 2013).

Emergent, floating-leaved, and submerged vegetation dominates the lowest elevations in the Wax Lake delta. *Nelumbo lutea* (American lotus) is an aquatic, perennial herb with round, flat leaves 30–60 cm in diameter that can be either floating or emergent. It grows from rhizomes rooted in the bottom of shallow water areas and stands are capable of rapid radial expansion of up to 14 m in a single growing season (Hall and Penfound 1944). Two *Sagittaria* spp. – *Sagittaria latifolia* and *Sagittaria platyphylla* – have historically been important components of the plant community in the Wax Lake delta, although their dominance appears to have waned in recent years (Holm and Sasser 2001). Both are emergent perennial herbs, but *S. latifolia* is taller, reaching mature heights of up to 1.5 m compared to less than 1 m for *S. platyphylla* (NRCS 2013). The leaves of *S. latifolia* are arrowhead-shaped whereas those of *S. platyphylla* are elliptical. No attempt was made to differentiate the two species for mapping purposes.

Finally, areas within the delta that are continuously flooded are dominated by floating plants and SAVs. *Eichhornia crassipes* (water hyacinth) is an invasive free-floating freshwater aquatic plant that forms dense mats over waterways, blocking light-penetration of the water column. Small, broken-off mats of *E. crassipes* are commonly found floating down the distributary channels in the Wax Lake Delta. It forms large mats in the interiors of the islands that are moved continuously by wind and tides. The most common SAV in the delta is *P nodosus* (longleaf pondweed). It is a rhyzomous perennial aquatic herb with linear leaves about 5 cm long that float at and just below the water's surface (NRCS 2013). Because its floating leaves prevent light from penetrating the water column, it often forms large homogeneous stands. This growth form gives it a unique spectral signature compared to other SAVs, which allowed it to be mapped as a separate class for this study. All other SAVs were grouped into a single class for mapping purposes. Other SAV species present in the delta include *Potamogeton pusillus*, *Potamogeton crispus*, *Myriophyllum spicatum*, *Elodea canadensis*, *Najas guadalupensis*, *Zannichellia palustris*, *Herteranthera dubbia*, and *Cerataphylum demersum*. These other species are frequently found in mixed assemblages throughout the delta (Charles Sasser, unpublished data).

2.3. Reference data

Training areas and a stratified random sample of accuracy assessment plots were collected in the field in late August and early September 2011. Training samples were collected as monotypic or nearly monotypic stands of each of the vegetation classes with polygons delineated using a Trimble GeoXH differential global positioning system (DGPS) with sub-metre accuracy. Accuracy assessment samples were collected by generating a stratified random sample of 400 points using a previously generated classification based on a

June 2010 WV-2 image of the Wax Lake delta. A total of 85 of these points were visited in the field, selected based on accessibility by foot or airboat, with the objective of obtaining adequate representation of each class. For classes that were poorly represented in the 2010 vegetation map (*Z. milacea*, *P. australis*), accessible stands were haphazardly selected in the field to include in the accuracy assessment. *Paspalum dissectum* was excluded from the accuracy assessment because it is found primarily in one isolated area of the delta and the reference plots were inaccessible, although sufficient non-random training samples were collected. *Eichhornia crassipes* was also excluded from the accuracy assessment because the floating mats of this species move continuously. At each accuracy assessment site, percentage cover values were collected at 5% intervals within a 1 m^2 sample plot, which was selected such that it was representative of the greater 5 m^2 area to account for the 2 m pixel size of the WV-2 data plus any geometric error in the GPS reading and image registration.

Use of these reference data for the 16 October 2011 WV-2 image was complicated by Tropical Storm Lee, which passed directly over the Wax Lake delta on 4 September 2011. This slow-moving storm brought an approximately 4 foot storm surge as measured at the Wax Lake delta Coastal Reference Monitoring System (CRMS) monitoring site maintained by the US Geological Survey and the Coastal Protection and Restoration Authority of Louisiana (CPRA 2012). This surge carried salt water into the delta that killed much of the freshwater vegetation growing at low elevations, as evidenced by widespread salt-burn observed in the delta in the weeks following the storm. In particular, four of the classes that normally dominate the low elevation areas of the delta – *N. lutea*, *Sagittaria* spp., *P. nodosus*, and other SAVs – were greatly reduced in distribution as a result of the storm, whereas the area of bare mud or sand flats was greatly increased. Because access to the site was limited for several months following the storm, all training areas collected before the storm were screened by visual interpretation of the 16 October 2011 WV-2 image, using a June 2010 WV-2 image and a reference vegetation map created from November 2009 aerial photography as ancillary data. If an insufficient number of the original training pixels for a given class were usable due to the storm impact, additional training pixels were selected directly from the image using the ancillary data as reference. To minimize training error, new training pixels were only selected from areas that were mapped as the same class in 2009 and 2010 and where visual interpretation of the 2011 image suggested the vegetation class had not changed. The storm also resulted in a conversion of a high number of accuracy assessment plots from the lower elevation classes to the 'bare sediment' class. Conversion of these sites was verified by visual interpretation of the 16 October 2011 WV-2 image. As it was impossible to obtain new reference samples for these classes following the storm, they were under-represented in the final accuracy assessment data set.

2.4. Classification

The November 2011 WV-2 image of the Wax Lake delta was first converted to at-satellite reflectance and then both MLC and SVM classifiers were tested to determine which classifier yielded the most accurate classification of freshwater marsh vegetation using the WV-2 high-resolution multispectral imagery. All classifications were performed using the ENVI 5.0 image analysis software package (Exelis VIS 2013). MLC is a very commonly used classifier for multispectral imagery due to its ease of implementation and wide availability in popular software packages. However, it assumes that reflectance values are normally distributed, an assumption that is commonly violated in remote-sensing data,

particularly where there are multiple subclasses or when classes contain different spectral features (Kavzoglu and Reis 2008). This problem has led to the recent proliferation of non-parametric classifiers such as classification trees, neural networks, and SVMs (Zhu and Blumberg 2002; Kavzoglu and Reis 2008; Otukei and Blaschke 2010; Friedl and Brodley 1997). Of these, SVMs have most often demonstrated superior thematic classification accuracy (Sanchez-Hernandez, Boyd, and Foody 2007; Huang, Davis, and Townshend 2002; Kavzoglu and Colkesen 2009; Dixon and Candade 2008; Pal and Mather 2005; Foody and Mathur 2004).

SVMs are a group of machine learning techniques based on statistical learning theory. They separate classes by identifying the optimal linear decision surface (the optimal hyperplane) that creates the largest distance, or margin, between the vectors for the two classes. In situations where the training sets for the classes are not linearly separable, the data must first be projected into a higher dimensional space where they are linearly separable (Pal and Mather 2005). This is most often accomplished using kernel functions, of which the polynomial and radial bias function (RBF) have been the most commonly adopted for remote-sensing applications (Kavzoglu and Colkesen 2009; Huang, Davis, and Townshend 2002). We tested both RBF and polynomial kernels to determine which provided superior classification accuracy. To determine the optimal parameters for this study area, classification trials were performed using parameter ranges used in previous studies in other settings (Kavzoglu and Colkesen 2009; Huang, Davis, and Townshend 2002; Pal and Mather 2005). For the RBF kernel, gamma was varied from 0.01 to 7 and the penalty parameter was varied from 10 to 10,000. For the polynomial kernel, polynomial order was varied from 2 to 6 and the penalty parameter was again varied from 10 to 10,000. The ENVI SVM classification module employs the pairwise approach to extend binary SVM classification to multiclass problems.

Apart from evaluating the value of the full eight-band imagery for mapping freshwater wetland vegetation, we also evaluated the contribution of the new coastal blue, yellow, and red-edge bands by performing MLC after sequentially removing each of these bands. Additional classifications were performed at degraded resolutions and with decreased band combinations to compare the results of the 2 m, eight-band WV-2 imagery to results obtainable using other high-resolution satellite sensors. To simulate IKONOS and OrbView-3 data, the WV-2 image was resampled to 4 m spatial resolution and only bands 2 (red), 3 (green), 5 (red), and 7 (near infrared) were used. The same band combination was used to simulate QuickBird data, but the image was resampled to 2.4 m.

Accuracy assessment results were summarized in an error matrix and overall map accuracy, kappa values, and individual class user's and producer's accuracies were computed based on the dominant class in each reference plot (Story and Congalton 1986; Stehman 1997; Richards 1996; Congalton 1991). The statistical significance of differences in overall map accuracy was tested using the McNemar test (Foody 2004).

3. Results

3.1. SVM parameter optimization

For the RBF SVM classification trials, varying gamma from 0.01 to 7.0 resulted in only a slight decrease in classification accuracy for gamma values greater than 1 (Figure 2). For gamma values below 1, overall classification accuracy was 68% (kappa = 0.63) and for gamma values above 1, overall accuracy dropped to 67% (kappa = 0.62). Accuracy among the vegetation classes remained constant at 55% (kappa = 0.48) for all values of

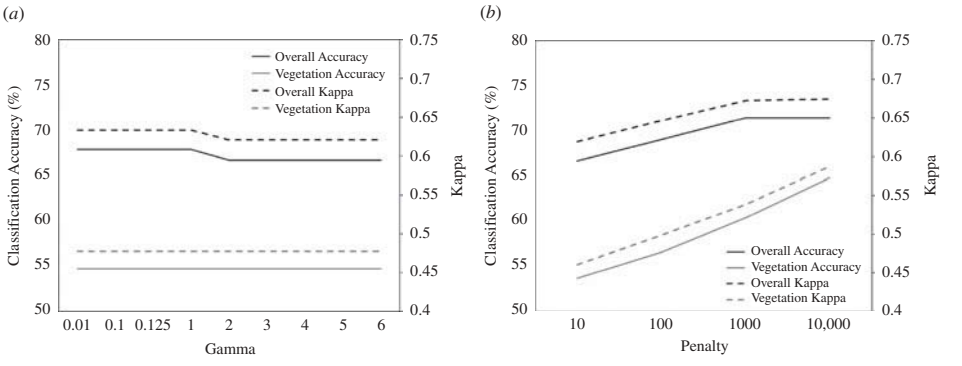

Figure 2. Optimization for RBF SVM classification: (*a*) results of Gamma optimization trials, (*b*) results of penalty optimization trials.

kappa tested (Figure 2(*a*)). Unsurprisingly, the McNemar test results indicated that there were no significant differences in classification accuracy among the kappa trials. The ENVI default kappa value of 0.125 was therefore selected for the remainder of the SVM classifications. Varying the penalty parameter resulted in a slight increase in classification accuracy from an overall accuracy of 67% (kappa = 0.62) when the penalty parameter was set to 10 to an overall accuracy of 71% (kappa = 0.67) when the penalty parameter was set to 10,000 (Figure 2(*b*)). There was a greater increase in the accuracy of the vegetation classes from 54% (kappa = 0.46) to 65% (kappa = 0.59) over the same range. However, the McNemar test results indicated that none of these differences in classification accuracy were significant at the 0.05 probability level.

For the polynomial SVM classification, varying the polynomial order from 2 to 6 resulted in an increase in overall classification accuracy from 67% (kappa = 0.62) to 71% (kappa = 0.67) and an increase in vegetation class accuracy from 55% (kappa = 0.48) to 63% (kappa = 0.57) (Figure 3(*a*)). The results of the McNemar tests indicated that differences in classification accuracy among SVM classifications with different polynomial orders were not significant at the 0.05 probability level. A polynomial order of 6 was selected for the remaining polynomial parameter trials because it resulted in the highest overall accuracy, although the differences in accuracy were not statistically significant.

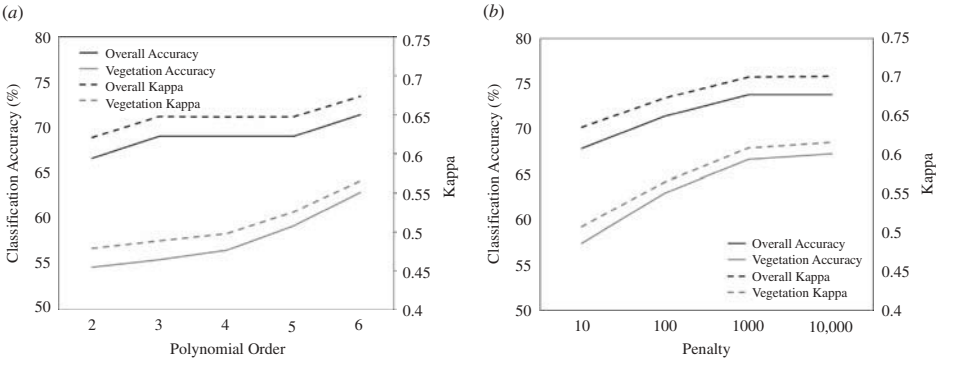

Figure 3. Optimization for polynomial SVM classification: (*a*) results of order optimization trials, (*b*) results of penalty optimization trials.

Varying the penalty parameter from 10 to 10,000 resulted in an increase in overall classification accuracy from 67.9 (kappa = 0.64) to 73.8 (kappa = 0.70) and an increase in vegetation class accuracy from 57.4 (kappa = 0.51) to 67.3 (kappa = 0.62) (Figure 3(*b*)). Based on the McNemar test, the classification accuracy was significantly greater using penalty values of 1000 or 10,000 as opposed to 10, but classification accuracy at a penalty value of 100 was not significantly different from the accuracies for smaller or larger penalty values.

Based on these trials, the highest overall classification accuracy of 73.8 was achieved for the SVM classification using the polynomial kernel with an order of 6 and a penalty value of 10,000.

3.2. *Comparing MLC and SVM classifications*

Overall classification accuracy for the MLC classification was 75%, with a kappa value of 0.71 (Table 1). When only the vegetation classes were considered, classification accuracy was 71.7% (kappa = 0.71). Producer's accuracy ranged from 0% for *B. laevis* to 100% for *P. punctatum*, *N. lute*a, and water. User's accuracy ranged from 0% for *B. laevis* to 100% for *C. esculenta*, *P. australis*, other SAVs, and water. User's accuracies greater than or equal to 70% were found for seven classes: *S. nigra* (89%), *C. esculenta* (100%), *Typha* spp. (75%), *P. australis* (100%), other SAVs (100%), water (100%), and bare/mudflat (93%). Producer's accuracies greater than or equal to 70% were found for the following six classes: *S. nigra* (89%), *P. punctatum* (100%), *N. lutea* (100%), other SAVs (75%), water (100%), and bare/mudflat (70%).

The confusion matrix for the MLC classification (Table 2) indicates that there is a high incidence of misclassification of other vegetation classes as *P. punctatum*. The classes most commonly confused with *P. punctatum* were *C. esculenta*, *Typha* spp., and

Table 1. Comparison of SVM and MLC classification accuracy.

	SVM		MLC	
Class	User's accuracy (%)	Producer's accuracy (%)	User's accuracy (%)	Producer's accuracy (%)
Salix nigra	81.8	100.0	88.9	88.9
Colocasia esculenta	88.9	66.7	100.0	66.7
Polygonum puncatum	56.3	81.8	50.0	100.0
Bidens laevis	NA	NA	0.0	0.0
Typha spp.	33.3	14.3	75.0	42.9
Zizaniopsis miliacea	16.7	33.3	25.0	33.3
Phragmites australis	50.0	50.0	100.0	50.0
Nelumbo lutea	71.4	100.0	60.0	100.0
Other SAVs	100.0	75.0	100.0	75.0
Water	100.0	100.0	100.0	100.0
Bare/mudflat	93.3	77.8	93.3	70.0
Overall accuracy (%)	**73.8**		**75.0**	
Kappa	**0.70**		**0.71**	
Vegetation accuracy (%)	**67.3**		**71.7**	
Vegetation kappa	**0.62**		**0.66**	

Table 2. Confusion matrix for MLC classification.

	Reference data												
	Salix nigra	*Colocasia esculenta*	*Polygonum punctatum*	*Bidens laevis*	*Typha* spp.	*Zizaniopsis miliacea*	*Phragmites australis*	*Nelumbo lutea*	*Eichhornia crassipes*	Other SAVs	Water	Bare/ mudflat	Total
Classification													
Salix nigra	**8**	1	0	0	0	0	0	0	0	0	0	0	9
Colocasia esculenta	0	**8**	0	0	0	0	0	0	0	0	0	0	8
Polygonum punctatum	0	3	**11**	1	3	2	0	0	0	0	0	2	22
Bidens laevis	1	0	0	**0**	0	0	0	0	0	0	0	0	1
Typha spp.	0	0	0	0	**3**	0	1	0	0	0	0	0	4
Zizaniopsis miliacea	0	0	0	0	0	**1**	0	0	0	0	0	3	4
Phragmites australis	0	0	0	0	0	0	**1**	0	0	0	0	0	1
Nelumbo lutea	0	0	0	0	0	0	0	**3**	0	1	0	1	5
Eichhornia crassipes	0	0	0	1	0	0	0	0	**0**	0	0	0	1
Other SAVs	0	0	0	0	0	0	0	0	0	**3**	0	0	3
Water	0	0	0	0	0	0	0	0	0	0	**11**	0	11
Bare/ mudflats	0	0	0	0	1	0	0	0	0	0	0	**14**	15
Total	9	12	11	2	7	3	2	3	0	4	11	20	**84**

Z. miliacea. Another frequent source of classification error was the misclassification of bare/mudflat areas as vegetation, particularly *Z. miliacea* and *P. punctatum*.

Overall classification accuracy for the best SVM classification was 71%, with a kappa value of 0.67. User's accuracies ranged from 14% for *Z. miliacea* to 100% for other SAVs and water. User's accuracies greater than 70% were found for the following five classes: *S. nigra* (82%), *C. esculenta* (89%), other SAVs (100%), water (100%), and bare/mudflat (93%). Producer's accuracies ranged from 14% for *Typha* spp. to 100% for *S. nigra*, *N. lutea*, and water. Six classes had producer's accuracies greater than 70%: *S. nigra* (100%), *P. punctatum* (73%), *N. lutea* (100%), other SAVs (75%), water (100%), and bare/mudflat (74%).

Although overall accuracy was higher for the MLC classification, the McNemar test results indicate that the difference in classification accuracy is not statistically significant. The two classifiers differed in their estimation of the areal extent of each of the vegetation classes. The MLC classification mapped greater areas of *Z. miliacea*, *P. nodosus*, *P. punctatum*, *P. australis*, *N. lutea*, and dead vegetation, whereas the SVM classification mapped greater areas of *S. nigra* seedlings, *Sagittaria* spp., *P. dissectum*, other SAVs, *E. crassipes*, and *C. esculenta* (Figures 4 and 5).

3.3. *Contribution of the new spectral bands*

Table 3 demonstrates the change in classification accuracy associated with each of the four new spectral bands employed by the WV-2 sensor. The exclusion of the red-edge band (band 6) had the greatest impact on classification accuracy, both at the level of

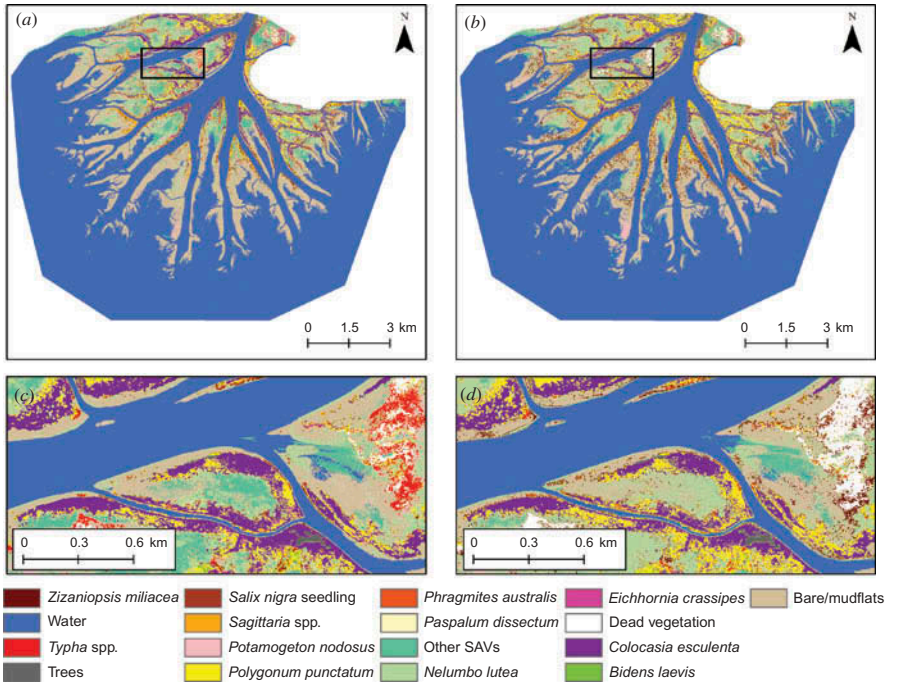

Figure 4. Comparison of SVM and MLC classification maps: (*a*) and (*c*) SVM classification, (*b*) and (*d*) MLC classification.

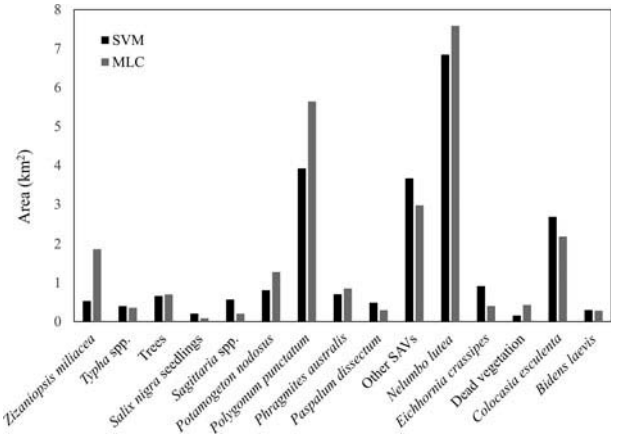

Figure 5. Distribution of area among classes for SVM and MLC classifications.

Table 3. Change in classification accuracy associated with the new bands in the WorldView-2 sensor.

	All classes		Vegetation classes	
Trial	Overall accuracy (%)	Kappa	Overall accuracy (%)	Kappa
All Eight Bands	75.0	0.71	71.7	0.66
Minus Band 1 (coastal blue)	71.4	0.67	66.0	0.60
Minus Band 4 (yellow)	75.0	0.71	71.7	0.66
Minus Band 6 (red-edge)	69.1	0.65	62.3	0.56
Minus Band 8 (IR)	73.8	0.70	69.8	0.64

overall accuracy and among the vegetation classes in particular. Removing this band decreased overall classification accuracy by approximately 6 percentage points and vegetation class accuracy by nearly 10 percentage points. The coastal blue band (band 1) had the second largest contribution to classification accuracy in this coastal deltaic system, with its removal resulting in a decrease in overall accuracy of 3.6 percentage points and a decrease in vegetation class accuracy of 5.7 percentage points. The second NIR band (band 8) contributed minimally to classification accuracy, with its removal resulting in only a 1.2 percentage point decrease in overall accuracy and a 1.9 percentage point decrease in vegetation class accuracy. Surprisingly, removing the yellow band (band 4) resulted in no decrease in either overall or vegetation class accuracy for this system. Although these differences in classification accuracy are substantial, the McNemar test results indicated that they are not statistically significant at the 0.05 significance level, both in comparison to the full eight-band WV-2 classification and among each other.

3.4. Comparison to other high-resolution sensors

Table 4 shows the results of comparison between the full eight-band WV-2 imagery and simulated imagery from the QuickBird, IKONOS, and OrbView-3 sensors. Reducing the WV-2 image to the four bands used by the QuickBird sensor and degrading the spatial

Table 4. Comparison to other high-resolution sensors.

	All classes		Vegetation classes	
Trial	Overall accuracy (%)	Kappa	Overall accuracy (%)	Kappa
All eight bands, 2 m (WorldView-2)	75.0	0.71	71.7	0.66
4 Band, 2.4 m (QuickBird)	70.2	0.66	62.3	0.56
4 Band, 4 m (IKONOS, OrbView-3)	69.1	0.64	58.5	0.51

resolution to 2.4 m resulted in a nearly 5 percentage point decrease in overall classification accuracy and a decrease of over 8 percentage points for the vegetation classes. Further degrading the spatial resolution to 4 m to simulate the IKONOS and OrbView-3 sensors resulted in an additional loss of 1 percentage point for overall accuracy and nearly 4 percentage points for vegetation class accuracy. The results of the McNemar tests indicated that the difference in classification accuracy between the reduced-band and degraded spatial resolution classifications was not significantly different from the classification based on the full eight-band WV-2 data at the 0.05 significance level.

4. Discussion

The results of these SVM classification kernel parameter trials differ from those of previous studies, highlighting the importance of optimizing the kernel parameters to each individual imagery source, study area, and classification task when performing SVM classification. In this study, we found that the polynomial kernel with an order of 6 and penalty value of 10,000 gave optimal results when using WV-2 satellite data to map vegetation at the species level in a deltaic, freshwater marsh setting with sharp species zonation. The different results obtained by authors of previous studies likely relate to differences in the number of available bands, spatial scale, and classification scale or degree of class heterogeneity in those studies. Huang, Davis, and Townshend (2002) found that the accuracy of SVM classification using the polynomial kernel increased as order increased from 1 to 8, similar to what was found in this study. They attributed this effect of polynomial order to the small number of variables (imagery bands) used in their studies. As this study also used few input bands compared to hyperspectral imagery, our results further support those conclusions. Huang, Davis, and Townshend (2002) observed an increase in classification accuracy using the RBF kernel when gamma was increased from 1 to 7.5. In this study, no significant impact of gamma on classification accuracy was observed over the same range of values.

Many previous studies have achieved the greatest classification accuracy with the SVM classifier using the RBF kernel. Pal and Mather (2005) found that the RBF kernel with a gamma value of 2 and penalty value of 5000 resulted in optimum classifier performance both for mapping agricultural crops using Landsat ETM+ data and for mapping broad land-cover classes (e.g. vineyards, hydrophytic vegetation, pasture, urban) using hyperspectral imagery. Kavzoglu and Colkesen (2009) also found that the RBF kernel provided superior classification accuracy for mapping broad land-cover classes using Landsat ETM+ and Terra ASTER imagery. They found that a gamma value of 3 and a penalty parameter of 250 were optimal for the RBF kernel using the Landsat ETM+ image but a gamma value of 1 and penalty parameter of 245 produced

optimal results using the ASTER imagery, further supporting the need to optimize each kernel to the specific imagery and classification task at hand. However, not all previous studies have favoured the RBF kernel – Dixon and Candade (2008) obtained optimal results for Landsat TM 5 data using the polynomial kernel with an order of 3 and penalty value of 1000, suggesting that optimal kernel choice is also highly variable among remote-sensing applications.

Our finding that the MLC classifier performed as well as or better than the SVM classifier differs from the findings of most other remote-sensing studies, in which SVM has been shown to be superior to MLC in a wide variety of settings and using imagery ranging from moderate-resolution satellite imagery (Landsat and ASTER) to high-resolution hyperspectral imagery (Huang, Davis, and Townshend 2002; Kavzoglu and Colkesen 2009; Dixon and Candade 2008; Pal and Mather 2005; Boyd, Sanchez-Hernandez, and Foody 2006). The source of this discrepancy likely lies in the statistical distribution of reflectance values in each spectral band for each of the target classes. The SVM classifier frequently outperforms the MLC classifier because it does not require that the reflectance values for the individual classes be normally distributed. Many mapped land-cover classes consist of multiple materials or subclasses with different spectral properties, resulting in bimodal or multimodal distributions. Bimodal or multimodal reflectance distributions are particularly common when coarse land-cover classes are used relative to the spatial resolution of the sensor. In this study, the plant species mapped grow in relatively monotypic stands, resulting in reflectance distributions that are better approximated by the Gaussian normal distribution (Figure 6). This makes use of the MLC classifier appropriate, particularly given its easier implementation compared to the SVM parameter, as it does not require kernel optimization. The classes that were poorly classified by the MLC classifier were those that either were potentially poorly trained due to Tropical Storm Lee (*Z. mileacea*, *Typha* spp.) or those that tend to grow in mixed stands with other unclassified species present as subdominants. The latter case is exemplified by

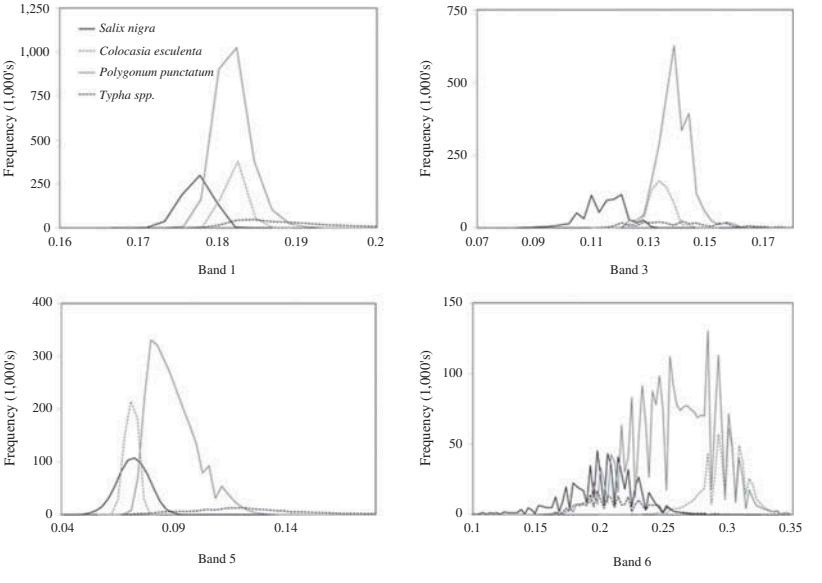

Figure 6. Histograms showing the distribution of reflectance values for *Salix nigra, Colocasia esculenta, Polygonum punctatum*, and *Typha* spp. in WV-2 bands 1, 3, 5, and 6.

P. punctatum, which was frequently over-mapped at the expense of *C. esculenta*, *Typha* spp., and *Z. mileacea*. The *P. punctatum* class is the most heterogeneous class included in the classification. Several unclassified species that are rarely dominant over large areas of the delta (e.g. *Leersia oryzoides*, *Panicum hemitomon*, *Vigna luteola*) are present as subdominants in the *Polygonum* community and can lead to classification error when they are also subdominant in other classes, particularly since they were more likely to be included in the training areas for *P. punctatum* than for the other classes. Closer examination of the misclassified accuracy assessment points indicates that most of the points misclassified as *P. punctatum* were highly mixed, with 40% or more combined cover values for unclassified subdominant species. *V. luteola* was also present at some of the misclassified sites. *V. luteola* is a vine that creates a dense layer covering the herbaceous marsh vegetation, blocking reflectance from the species that would be considered dominant based on cover values alone. It is therefore unsurprising that the presence of this species would increase classification error and future mapping studies should include this species as a separate vegetation class.

The results of this study compare favourably to other studies where high-resolution satellite imagery has been used to map coastal vegetation. Collin and Planes (2011) achieved kappa values greater than 0.9 for both artificial neural network (ANN) and SVM classification of WV-2 imagery, including specific tree species as well as broader vegetation classes such as 'bush' and 'grass'. The lower classification accuracy in this study is most likely due to our nearly exclusive focus on individual species, without the inclusion of broader mixed classes. Whereas overall classification accuracy and kappa values were diminished by several classes that might have been poorly trained due to interference by Tropical Storm Lee, class-specific user's and producer's accuracies greater than 90% were found for several species. Immitzer, Atzberger, and Koukal (2012) similarly found user's accuracies ranging from 57% to 92% and producer's accuracies ranging from 33% to 94% for individual tree species using WV-2 data. Belluco et al. (2006) achieved overall accuracies of greater than 95% when classifying salt marsh species using high spatial resolution QuickBird and IKONOS imagery. However, salt marsh plant zonation tends to be much stricter along tidal inundation gradients than the zonation observed among freshwater species in the Wax Lake delta, allowing for greater species-level classification accuracy. The accuracies achieved in this study also compare favourably to the accuracies achieved for species-specific classifications using hyperspectral imagery (Belluco et al. 2006; Filippi and Jensen 2006; Hirano, Madden, and Welch 2003), but at significantly reduced cost.

In general, bands 1 (coastal blue), 6 (red-edge), and 8 (second IR) resulted in slight increases in overall classification accuracy compared to trials where they were removed prior to classification, although the differences in classification accuracy were not statistically significant based on the McNemar test. The red-edge band contributed the most to both increased overall classification accuracy and accuracy of the vegetation classes, specifically. Unsurprisingly, its impact was greater on vegetation class accuracy than on overall accuracy. Previous studies have indicated that spectral information in the red-edge portion of the light spectrum may be particularly valuable for separating coastal marsh species (Artigas and Yang 2006), and our results support that assertion. The coastal blue band was second in terms of its contribution of increased accuracy, followed by the second IR band. Removal of the yellow band, however, resulted in no change in classification accuracy for this particular application. This is surprising because the yellow band corresponds to the absorption band for minor plant pigments that become more important during senescence and the image use for this analysis was taken in October.

However, the growing season is quite long in coastal Louisiana with the average first fall freeze not occurring until early December (LOSC and SRCC 2013). It is possible that the influence of the yellow band would be more apparent for imagery taken during November or December, in this particular climate.

The additional four bands in the WV-2 sensor do appear to provide greater discriminating power for freshwater wetland vegetation compared to other available 4-band high-resolution satellite sensors such as QuickBird, IKONOS, and OrbView-3. The inclusion of the four additional bands resulted in a 5% increase in overall accuracy, compared to the spectrally degraded data set, and a 9.4% increase in accuracy among the vegetation classes. The enhanced spatial resolution of the WV-2 sensor is less important for mapping coastal marsh vegetation at the species-level – spatially degrading the data set to 4 m spatial resolution to mimic IKONOS and OrbView-3 resulted in only a marginal decrease in classification accuracy compared to the spectrally reduced 2 m data set designed to mimic Quickbird. Overall, these results indicate that WV-2 imagery provides better results for mapping the distribution of freshwater marsh species than other available high-resolution satellite sensors, largely as a result of the addition of the red-edge and, to a lesser extent, the coastal blue bands.

5. Conclusions

As this study demonstrates, the combination of eight spectral bands of information and high spatial resolution makes the new WV-2 satellite well suited to mapping diverse and heterogeneous coastal wetland systems such as the Wax Lake delta. An overall classification accuracy of 75% was achieved and individual user's and producer's accuracies greater than 70% were achieved for many species. These accuracies exceed species-specific mapping results found using four-band high-resolution satellite sensors such as IKONOS and QuickBird and rivals those found using satellite and airborne hyperspectral sensors but at lower acquisition cost and with reduced processing time and effort. The red-edge and coastal blue bands contributed the most to increased mapping accuracy and the combination of all eight spectral bands provided greater classification accuracy than when only the four more common bands were used. Surprisingly, the exclusion of the yellow band had no impact on classification accuracy in this instance. This is likely because most of the mapped plant species had not yet begun to senesce at the time of image acquisition. Further studies performed using imagery timed to maximize variability in the degree of senescence between species would provide a better measure of the potential benefit of this band.

Contrary to several previous studies, the parametric MLC classifier provided as high or higher map accuracy than the non-parametric SVM classifier for this particular mapping application. The favourable performance of the MLC classifier in this study is likely a result of the fairly homogenous composition of the target classes at the 2 m spatial scale and hence relatively normal distribution of the reflectance values for each class in each of the spectral bands. The SVM classifier has become increasingly popular due to its ability to handle remote-sensing data that violate the assumption of normality that is implicit in parametric classifiers such as MLC. However, the SVM classifier requires substantially more effort due to the need to optimize kernel and parameter selection for each remote-sensing application and computing time can be extensive depending on the parameter values selected and the resolution of the imagery. The results of this study suggest that the simpler MLC classifier is adequate for mapping individual plant species using high spatial resolution imagery in a river delta setting with a high degree of species zonation.

Acknowledgements

The authors would like to thank the Louisiana Center for Geoinformatics for providing the GPS equipment used for this study and assisting with differential correction. We also thank Brian Milan for assistance with fieldwork and Elaine Hebert for providing reference maps and expertise in image interpretation.

Funding

This work was supported by a Louisiana Board of Regents fellowship to Melissa Carle.

References

Adam, E., O. Mutanga, and D. Rugege. 2010. "Multispectral and Hyperspectral Remote Sensing for Identification and Mapping of Wetland Vegetation: A Review." *Wetlands Ecology and Management* 18: 281–296. doi:10.1007/s11273-009-9169-z.

Artigas, F. J., and J. Yang. 2006. "Spectral Discrimination of Marsh Vegetation Types in the New Jersey Meadowlands, USA." *Wetlands* 26 (1): 271–277. doi:10.1672/0277-5212(2006)26[271:SDOMVT]2.0.CO;2.

Belluco, E., M. Camuffo, S. Ferrari, L. Modenese, S. Silvestri, A. Marani, and M. Marani. 2006. "Mapping Salt-Marsh Vegetation by Multispectral and Hyperspectral Remote Sensing." *Remote Sensing of Environment* 105 (1): 54–67. doi:10.1016/j.rse.2006.06.006.

Boyd, D. S., C. Sanchez-Hernandez, and G. M. Foody. 2006. "Mapping a Specific Class for Priority Habitats Monitoring from Satellite Sensor Data." *International Journal of Remote Sensing* 27 (13): 2631–2644. doi:10.1080/01431160600554348.

Carter, G. A. 1993. "Responses of Leaf Spectral Reflectance to Plant Stress." *American Journal of Botany* 80 (3): 239–243. doi:10.2307/2445346.

Carter, G. A., W. G. Cibula, and R. L. Miller. 1996. "Narrow-Band Reflectance Imagery Compared with Thermal Imagery for Early Detection of Plant Stress." *Journal of Plant Physiology* 148 (5): 515–522. doi:10.1016/S0176-1617(96)80070-8.

Chabreck, R. H., and R. E. Condrey. 1979. *Common Vascular Plants of the Louisiana Marsh*. Baton Rouge, LA: Louisiana Sea Grant Publication Number LSU-T-79-003.

Cohen, J. E., C. Small, A. Mellinger, J. Gallup, J. Sachs, P. M. Vitousek, and H. A. Mooney. 1997. "Estimates of Coastal Populations." *Science* 278 (5341): 1209–1213. doi:10.1126/science.278.5341.1209c.

Collin, A., and J. L. Hench. 2012. "Towards Deeper Measurements of Tropical Reefscape Structure Using the WorldView-2 Spaceborne Sensor." *Remote Sensing* 4 (12): 1425–1447. doi:10.3390/rs4051425.

Collin, A., and S. Planes. 2011. "What Is the Value Added of 4 Bands within the Submetric Remote Sensing of Tropical Coastscape? Quickbird-2 vs WorldView-2." In *IEEE International Geoscience and Remote Sensing Symposium*, July 24–29, Vancouver, 2165–2168. Vancouver, BC: The Institute of Electrical and Electronics Engineers.

Congalton, R. G. 1991. "A Review of Assessing the Accuracy of Classifications of Remotely Sensed Data." *Remote Sensing of Environment* 37 (1): 35–46. doi:10.1016/0034-4257(91)90048-B.

Costanza, R., S. C. Farber, and J. Maxwell. 1989. "Valuation and Management of Wetland Ecosystems." *Ecological Economics* 1 (4): 335–361. doi:10.1016/0921-8009(89)90014-1.

CPRA (Coastal Protection and Restoration Authority of Louisiana) 2012. "Coastwide Reference Monitoring System – Wetlands Monitoring Data." Retrieved from the Strategic Online Natural Resource Information System (SONRIS) database. Accessed November 9. www.lacoast.gov/crms.

Crossett, K. M., T. J. Culliton, P. C. Wiley, and T. R. Goodspeed. 2004. *Population Trends along the Coastal United States: 1980–2008*. Silver Spring, MD: US Department of Commerce, National Oceanic and Atmospheric Administration.

Dixon, B., and N. Candade. 2008. "Multispectral Landuse Classification Using Neural Networks and Support Vector Machines: One or the Other, or Both?" *International Journal of Remote Sensing* 29 (4): 1185–1206. doi:10.1080/01431160701294661.

Doumlele, D. G. 1981. "Primary Production and Seasonal Aspects of Emergent Plants in a Tidal Freshwater Marsh." *Estuaries and Coasts* 4 (2): 139–142. doi:10.2307/1351676.

Exelis VIS. 2013. *Envi Version 5.0.* Herndon, VA: Exelis Visual Information Services.

Farber, S. C. 1987. "The Value of Coastal Wetlands for Protection of Property against Hurricane Wind Damage." *Journal of Environmental Economics and Management* 14: 143–151. doi:10.1016/0095-0696(87)90012-X.

Filippi, A. M., and J. R. Jensen. 2006. "Fuzzy Learning Vector Quantization for Hyperspectral Coastal Vegetation Classification." *Remote Sensing of Environment* 100: 512–530. doi:10.1016/j.rse.2005.11.007.

Foody, G., and A. Mathur. 2004. "A Relative Evaluation of Multiclass Image Classification by Support Vector Machines." *IEEE Transactions on Geoscience and Remote Sensing* 42 (6): 1335–1343. doi:10.1109/TGRS.2004.827257.

Foody, G. M. 2004. "Thematic Map Comparison: Evaluating the Statistical Significance of Differences in Classification Accuracy." *Photogrammetric Engineering and Remote Sensing* 70 (5): 627–633. doi:10.14358/PERS.70.5.627.

Friedl, M. A., and C. E. Brodley. 1997. "Decision Tree Classification of Land Cover from Remotely Sensed Data." *Remote Sensing of Environment* 61 (3): 399–409. doi:10.1016/S0034-4257(97)00049-7.

Gates, D. M., H. J. Keegan, J. C. Schleter, and V. R. Weidner. 1965. "Spectral Properties of Plants." *Applied Optics* 4 (1): 11–20. doi:10.1364/AO.4.000011.

Gitelson, A. A., and M. N. Merzlyak. 1994. "Quantitative Estimation of Chlorophyll-*a* Using Reflectance Spectra: Experiments with Autumn Chestnut and Maple Leaves." *Journal of Photochemistry and Photobiology B: Biology* 22 (3): 247–252. doi:10.1016/1011-1344(93)06963-4.

Gitelson, A. A., M. N. Merzlyak, and H. K. Lichtenthaler. 1996. "Detection of Red Edge Position and Chlorophyll Content by Reflectance Measurements near 700 nm." *International Journal of Remote Sensing* 148 (3–4): 501–508. doi:10.1016/S0176-1617(96)80285-9.

Hall, T. F., and W. T. Penfound. 1944. "The Biology of the American Lotus, Nelumbo Lutea (Wild.) Pers." *American Midland Naturalist* 31 (3): 744–758. doi:10.2307/2421417.

Hirano, A., M. Madden, and R. Welch. 2003. "Hyperspectral Image Data for Mapping Wetland Vegetation." *Wetlands* 23 (2): 436–448. doi:10.1672/18-20.

Holm, G. O., and C. E. Sasser. 2001. "Differential Salinity Response between Two Mississippi River Subdeltas: Implications for Changes in Plant Composition." *Estuaries* 24 (1): 78–89. doi:10.2307/1352815.

Hopkinson Jr, C. S. 1985. "Shallow-water Benthic and Pelagic Metabolism: Evidence of Heterotrophy in the Nearshore Georgia Bight." *Marine Biology* 87: 19–32. doi:10.1007/BF00397002.

Huang, C., L. S. Davis, and J. R. G. Townshend. 2002. "An Assessment of Support Vector Machines for Land Cover Classification." *International Journal of Remote Sensing* 23 (4): 725–749. doi:10.1080/01431160110040323.

Immitzer, M., C. Atzberger, and T. Koukal. 2012. "Tree Species Classification with Random Forest Using Very High Spatial Resolution 8-Band WorldView-2 Satellite Data." *Remote Sensing* 4 (12): 2661–2693. doi:10.3390/rs4092661.

Jackson, R. D. 1986. "Remote Sensing of Biotic and Abiotic Plant Stress." *Annual Review of Phytopathology* 24: 265–287. doi:10.1146/annurev.py.24.090186.001405.

Jensen, J. R. 2007. *Remote Sensing of the Environment: An Earth Resource Perspective*. 2nd ed. Upper Saddle River, NJ: Pearson Education.

Johnson, W. B., C. E. Sasser, and J. G. Gosselink. 1985. "Succession of Vegetation in an Evolving River Delta, Atchafalaya Bay, Louisiana." *The Journal of Ecology* 73 (3): 973–986. doi:10.2307/2260162.

Kavzoglu, T., and I. Colkesen. 2009. "A Kernel Functions Analysis for Support Vector Machines for Land Cover Classification." *International Journal of Applied Earth Observation and Geoinformation* 11 (5): 352–359. doi:10.1016/j.jag.2009.06.002.

Kavzoglu, T., and S. Reis. 2008. "Performance Analysis of Maximum Likelihood and Artificial Neural Network Classifiers for Training Sets with Mixed Pixels." *GIScience & Remote Sensing* 45 (3): 330–342. doi:10.2747/1548-1603.45.3.330.

Knutson, P. L., R. A. Brochu, W. N. Seelig, and M. R. Inskeep. 1982. "Wave Damping In *Spartina alterniflora* Marshes." *Wetlands* 2 (1): 87–104. doi:10.1007/BF03160548.

Knutson, P. L., J. C. Ford, M. R. Inskeep, and J. Oyler. 1981. "National Survey of Planted Salt Marshes (Vegetative Stabilization and Wave Stress)." *Wetlands* 1 (1): 129–157. doi:10.1007/BF03160460.

Llewellyn, D. W., and G. P. Shaffer. 1993. "Marsh Restoration in the Presence of Intense Herbivory: The Role of *Justicia lanceolata* (Chapm.) Small." *Wetlands* 13 (3): 176–184. doi:10.1007/BF03160878.

LOSC (Louisiana Office of State Climatology) and SRCC (Southern Regional Climate Center) 2013. "First Fall Freeze Dates." Accessed August 21. http://www.losc.lsu.edu/products/images/fall_freeze_50.gif

Marchisio, G., F. Pacifici, and C. Padwick. 2010. "On the Relative Predictive Value of the New Spectral Bands in the Worldwiew-2 Sensor." Paper presented at the IEEE international geoscience and remote sensing symposium, Honolulu, HI, July 25–30.

Nixon, S. W. 1980. "Between Coastal Marshes and Coastal Waters – A Review of Twenty Years of Speculation and Research on the Role of Salt Marshes in Estuarine Productivity and Water Chemistry." In *Estuarine and Wetland Processes*, edited by P. Hamilton and K. B. Macdonald, 437–525. New York: Plenum Press.

NRCS (United States Department of Agriculture, Natural Resource Conservation Service) 2013. "Plants Database." Accessed July 31. http://plants.usda.gov/java/

Odum, W. E. 1988. "Comparative Ecology of Tidal Freshwater and Salt Marshes." *Annual Review of Ecology and Systematics* 19: 147–176. doi:10.1146/annurev.es.19.110188.001051.

Otukei, J. R., and T. Blaschke. 2010. "Land Cover Change Assessment Using Decision Trees, Support Vector Machines and Maximum Likelihood Classification Algorithms." *International Journal of Applied Earth Observation and Geoinformation* 12: S27–S31. doi:10.1016/j.jag.2009.11.002.

Ozesmi, S. L., and M. E. Bauer. 2002. "Satellite Remote Sensing of Wetlands." *Wetlands Ecology and Management* 10: 381–402. doi:10.1023/A:1020908432489.

Pal, M., and P. M. Mather. 2005. "Support Vector Machines for Classification in Remote Sensing." *International Journal of Remote Sensing* 26 (5): 1007–1011. doi:10.1080/01431160512331314083.

Pasternack, G. B., W. B. Hilgartner, and G. S. Brush. 2000. "Biogeomorphology of an Upper Chesapeake Bay River-Mouth Tidal Freshwater Marsh." *Wetlands* 20 (3): 520–537. doi:2.0.CO;2",1,0,0>10.1672/0277-5212(2000)020<0520:BOAUCB>2.0.CO;2.

Richards, J. A. 1996. "Classifier Performance and Map Accuracy." *Remote Sensing of Environment* 57 (3): 161–166. doi:10.1016/0034-4257(96)00038-7.

Roberts, H. H., N. Walker, R. Cunningham, G. P. Kemp, and S. Majersky. 1997. "Evolution of Sedimentary Architecture and Surface Morphology: Atchafalaya and Wax Lake Deltas, Louisiana (1973–1994)." *Transactions of the Gulf Coast Association of Geological Societies* 47: 477–484.

Sanchez-Hernandez, C., D. S. Boyd, and G. M. Foody. 2007. "Mapping Specific Habitats from Remotely Sensed Imagery: Support Vector Machine and Support Vector Data Description Based Classification of Coastal Saltmarsh Habitats." *Ecological Informatics* 2 (2): 83–88. doi:10.1016/j.ecoinf.2007.04.003.

Shaffer, G. P., C. E. Sasser, J. G. Gosselink, and M. Rejmanek. 1992. "Vegetation Dynamics in the Emerging Atchafalaya Delta, Louisiana, USA." *The Journal of Ecology* 80 (4): 677–687. doi:10.2307/2260859.

Silva, T. S. F., M. P. F. Costa, J. M. Melack, and E. M. L. M. Novo. 2008. "Remote Sensing of Aquatic Vegetation: Theory and Applications." *Environmental Monitoring and Assessment* 140: 131–145. doi:10.1007/s10661-007-9855-3.

Simpson, R. L., R. E. Good, M. A. Leck, and D. F. Whigham. 1983. "The Ecology of Freshwater Tidal Wetlands." *Bioscience* 33 (4): 255–259. doi:10.2307/1309038.

Stehman, S. V. 1997. "Selecting and Interpreting Measures of Thematic Classification Accuracy." *Remote Sensing of Environment* 62 (1): 77–89. doi:10.1016/S0034-4257(97)00083-7.

Story, M., and R. G. Congalton. 1986. "Accuracy Assessment: A User's Perspective." *Photogrammetric Engineering and Remote Sensing* 52 (3): 397–399.

Whigham, D. F., and R. L. Simpson. 1992. "Annual Variation in Biomass and Production of a Tidal Freshwater Wetland and Comparison with Other Wetland Systems." *Virginia Journal of Science* 43 (1): 8–14.

Zhu, G., and D. G. Blumberg. 2002. "Classification Using ASTER Data and SVM Algorithms; The Case Study of Beer Sheva, Israel." *Remote Sensing of Environment* 80: 233–240. doi:10.1016/S0034-4257(01)00305-4.